Eq. (A8) can be written as

$$I=-\frac{2}{\pi v_e^3 v_i^3}\int_0^\infty dv\, v^2\int_0^v dv' v'^2[S\exp(-av^2-a'v'^2) +S'\exp(-a'v^2-av'^2)], \quad \text{(A11)}$$

where $a=1/(2v_e^2)$, $a'=1/(2v_i^2)$, and $S'(v,v')=S(v',v)$. The result of simplifying S and S' is to take Eq. (A11) to

$$I=-(8/3\pi v_e^3 v_i^3)(1-1/T)[\alpha(1,4)+\beta(4,1)], \quad \text{(A12)}$$

where

$$\alpha(m,n)=\int_0^\infty dv\int_0^v dv' v^m v'^n \exp(-av^2-a'v'^2) \quad \text{(A13)}$$

and $\beta(m,n)$ is obtained from $\alpha(m,n)$ by simply interchanging a and a'. Finally on using the relation

$$\int_0^\infty dy\, ye^{-sy^2}\,\mathrm{erf}(a^{1/2}y)=\frac{(a\pi)^{1/2}}{4s(a+s)^{1/2}},$$

we obtain

$$I=-\frac{(1-1/T)}{2\pi^{1/2}v_e^3v_i^3}\left[\frac{1}{aa'^2(a+a')^{1/2}}-\frac{1}{a'^2(a+a')^{3/2}} -\frac{1}{a'(a+a')^{5/2}}+\frac{1}{aa'^{5/2}}-\frac{1}{a(a+a')^{5/2}}\right]. \quad \text{(A14)}$$

As done in the text, if we neglect terms of the order (v_i^2/v_e^2), then Eq. (A6) with the help of Eq. (A14) gives

$$\frac{d\phi}{dt}\cong-\frac{2^{3/2}N\Gamma_e v_i^2}{3v_e^5\pi^{1/2}}\left(1-\frac{1}{T}\right), \quad \text{(A15)}$$

which in terms of the electron collision frequency ν_c can be rewritten as

$$\frac{1}{\omega_{pi}}\frac{d\phi}{dt}=\frac{2^{3/2}}{3\pi^{1/2}}\left(\frac{\nu_c}{\omega_{pi}}\right)\left(\frac{m}{M}\right)(1-T). \quad \text{(A16)}$$

In case of weak collisions, $(\nu_c/\omega_{pi})\ll 1$, so $(d\phi/dt)$ is negligible and thus Eq. (1) holds good to a very good approximation.

PHYSICAL REVIEW VOLUME 165, NUMBER 1 5 JANUARY 1968

Computer "Experiments" on Classical Fluids. II. Equilibrium Correlation Functions*

LOUP VERLET†
Belfer Graduate School of Science, Yeshiva University, New York, New York
(Received 21 July 1967)

Equilibrium correlation functions for a dense classical fluid are obtained by integrating the equation of motion of a system of 864 particles interacting through a Lennard-Jones potential. The behavior of the correlation function at large distance, and that of its Fourier transform at large wave number, are discussed in detail and shown to be related to the existence of a strong repulsion in the potential. A simple hard-sphere model is shown to reproduce very well the Fourier transform of those correlation functions at high density, the only parameter of the model being the diameter a of the hard spheres.

I. INTRODUCTION

USING a technique directly inspired by the beautiful work of Rahman,[1] we have performed some experiments on a classical fluid composed of 864 molecules interacting through a Lennard-Jones potential $V(r)=4\epsilon[(\sigma/r)^{12}-(\sigma/r)^6]$ cut at $r_v=2.5\sigma$ or $r_v=3.3\sigma$. The details of these computations and a discussion of the thermodynamical results have been given elsewhere.[2] Here we give a discussion of the pair function $g(r)$ and of the various quantities which can be derived from it, namely its Fourier transform and the direct correlation function.

We discuss in Sec. II the pair function as given by the machine computation. Some comparisons are made with the results of the integral equations. The maximum of $g(r)$ is seen to be a compromise between the tendency of the particles to cluster around the core of the potential at high density and the attraction due to the bowl of the potential, which plays an essential role at low temperature. These results would be meager if it were not possible to extend them (Sec. III). Firstly, it is shown that the effect of the tail of the potential, for $r>r_v$, which has been neglected in the molecular-dynamics calculation, would not have changed $g(r)$ appreciably for $r<r_v$ if it had been included. The results can thus be extended to an uncut potential. Secondly, a procedure is constructed to extrapolate $g(r)$

* Supported by the U. S. Air Force Office of Scientific Research, Grant No. 508-66.
† Permanent address: Laboratoire de Physique Théorique et Hautes Energies, Bâtiment 211, Faculté des Sciences, 91-Orsay, France.
[1] A. Rahman, Phys. Rev. **136**, A405 (1964).
[2] L. Verlet, Phys. Rev. **159**, 98 (1967).

to any r, and its practical validity is proven. Let us define, as usual, the direct correlation $c(r)$ through the Ornstein-Zernicke relation:

$$h(r)=c(r)+\rho\int h(r')c(|\mathbf{r}-\mathbf{r}'|)d\mathbf{r}', \tag{1}$$

where $h(r)=g(r)-1$ is the correlation function and ρ is the particle density. In all our "experiments" we can find some $r_c\leqslant r_v$ such that, for $r>r_c$, $h(r)$ is small. Then, presumably, a functional expansion[3] in $h(r)$ is reasonable and one can write, for $r>r_c$, the Percus-Yevick (PY) equation[4]

$$c(r)=g(r)(e^{\beta V(r)}-1). \tag{2}$$

For $r<r_c$, $g(r)$ is known from molecular dynamics, and the Ornstein-Zernicke relation (1) enables us to continue $g(r)$ outwards and $c(r)$ inwards. The validity of this procedure, which is the one we have used in general, is demonstrated by showing the insensitivity of the results to the chosen value of r_c.

More simply, when r_c is large enough, $c(r)$ may be simply replaced by

$$f(r)=\exp[-\beta V(r)]-1. \tag{3}$$

The direct correlation function which is thus found behaves as expected (Sec. IV). For $r\leqslant\sigma$ it resembles the function for the hard-sphere gas in the PY approximation.[5] It rises steeply around $r=\sigma$, and from then on looks very much like $f(r)$, although it is somewhat smaller, the more so if the density is high and the temperature small.

The use of the PY equation to get the potential once $g(r)$ and $c(r)$ are known can be put to a direct test. The Lennard-Jones potential would be recovered if the PY equation were exact. The results obtained show that at densities around that of the critical point[6] ($\rho<0.5$) the Lennard-Jones potential is recovered within a few percent. The results derived from the x-ray diffraction experiment at that density cannot be explained by a failure of that equation.[7] On the other hand, the error entailed by its use rises very rapidly. Its application in the very dense states such as those encountered in liquid metals is certainly not advisable.

In the next section (IV), we examine the position of the first peak k_0 of the Fourier transform of the correlation functions

$$\tilde{h}(k)=\rho\int e^{-i\mathbf{k}\cdot\mathbf{r}}h(r)d\mathbf{r}. \tag{4}$$

This is also the first peak of the Fourier transform $\tilde{c}(k)$ of the direct correlation function. It is shown qualitatively why we expect k_0 to be of the order of $2\pi/\sigma$, irrespective of the state. The slight dependence on the state, mainly on the density, is exhibited, and a comparison is made with the case of the hard-sphere gas and with experiment. These considerations make it likely that the location of the first peak is essentially a geometrical, excluded-volume effect.

This produces what is usually described by the concept of "short-range order". It is shown in Sec. VI that at high density $h(r)$ behaves effectively as a damped sine wave of period $r_0=2\pi/k_0$. More generally the relation between the behavior of $h(r)$ at large r and the dominant poles of $\tilde{h}(k)$ and $\tilde{c}(k)$ is analyzed in that section.[8]

The behavior of $\tilde{h}(k)$ for large k is then considered (Sec. VII). It is shown that this behavior is related to the first peak of $g(r)$, and that the oscillations of $\tilde{h}(k)$ are determined by the repulsive part of the potential. $\tilde{h}(k)$ behaves to a good approximation as $C\cos kr_w\, e^{-\alpha k}/k$, where r_w is of the order of σ. The parameters C, r_w, and α are studied in more detail: The rules deduced from the molecular-dynamics experiment, although purely descriptive in nature, may be of use in dealing with x-ray or neutron scattering experiments.

Lastly (Sec. VIII) a hard-sphere model of dense fluids is introduced as an illustration of some of the considerations underlying this article. This model, based on the Wertheim-Thiele solution[5] of the hard-sphere problem, is a generalization of the model which has been introduced by Ashcroft and Lekner,[9] to describe, in a quite satisfactory manner, the structure factor of liquid metals.

II. CORRELATION FUNCTION OBTAINED FROM MOLECULAR DYNAMICS

At each of the 1200 steps of the time integration of the equation of motion, all the distances which are smaller than r_v are recorded in special counters. The step in r used to calculate $g(r)$ is 0.04. The error on $g(r)$ may be estimated by comparing two independent runs made at the same values of the temperature and density: it is of the order of 1% at most. The values of the pressure and of the internal energy calculated from those correlation functions are in good agreement with those yielded by direct averages of the virial and of the potential energy,[2] although it should be realized that the step size in r for $g(r)$ is rather large: As the pressure depends sensitively on $g(r)$, some discrepancies arise; the error on $\beta p/\rho$ when calculated from $g(r)$ may reach 0.2 at the highest density considered. It is much smaller at lower density. Some examples are given in Table I.

[3] J. K. Percus, Phys. Rev. Letters **8**, 462 (1962).
[4] J. K. Percus and G. J. Yevick, Phys. Rev. **110**, 1 (1958).
[5] M. S. Wertheim, Phys. Rev. Letters **10**, 321 (1963); E. J. Thiele, J. Chem. Phys. **38**, 1959 (1963).
[6] We use the usual reduced units: $\sigma=\epsilon/k=1$.
[7] P. G. Mikolaj and C. J. Pings, Phys. Rev. Letters **15**, 849 (1965); J. Chem. Phys. **46**, 1401 (1967); *ibid.* **46**, 1412 (1967).
[8] The analysis of $g(r)$ for large r's in terms of poles of $\tilde{h}(k)$ is obviously not new. See e.g. J. G. Kirkwood and E. Monroe Boggs, J. Chem. Phys. **10**, 394 (1942); and, for a recent and rigorous analysis in the case of a repulsive interaction: J. Groenwoeld, paper given at the Copenhagen Conference on Statistical Mechanics, 1966 (unpublished).
[9] N. W. Ashcroft and J. Lekner, Phys. Rev. **145**, 83 (1966).

TABLE I. Test of the procedure used to extrapolate $g(r)$ beyond the cutoff distance r_c. In the first column is given the formula (see Sec. I) used to express $c(r)$ for $r>r_c$. The cutoff is made at the ith zero of $h(r)$; i is given in the second column. For the state (1), $T=1.07$, $\rho=0.75$. For the state (2), $T=0.88$, $\rho=0.85$. For the state (3), $T=2.202$, $\rho=0.85$. For those three states, $\beta p/\rho$ computed directly in the molecular dynamics is equal respectively to 0.90, 1.64, 4.20. The last line gives the results obtained using the PY Eq. (2) for all values of r.

$c(r)$ for $r>r_c$	i	state (1) $\beta p/\rho$	state (1) $\beta\partial p/\partial\rho$	state (1) $\tilde{h}(k_0)$	state (2) $\beta p/\rho$	state (2) $\beta\partial p/\partial\rho$	state (2) $\tilde{h}(k_0)$	state (3) $\beta p/\rho$	state (3) $\beta\partial p/\partial\rho$	state (3) $\tilde{h}(k_0)$
(2)	2	0.94	11.1	1.08	1.80	26.9	1.65	4.28	19.5	1.06
(2)	3	0.93	11.1	1.09	1.81	25.1	1.66	4.29	20.0	1.06
(2)	4	0.93	12.1	1.08	1.81	26.9	1.64	4.29	22.5	1.06
(3)	2	0.92	5.0	1.09	1.80	14.6	1.65	4.28	17.9	1.06
PY equation		1.69	5.6	1.04	3.18	10.5		4.23	15.3	1.07

In Fig. 1, we give a first example of such a calculation, as well as a comparison with the results obtained using the PY II equation,[10] relative to the state $T=1.46$, $\rho=0.4$. It is seen that at that density, slightly above critical, the PY II equation still works quite well. This is evident both from the direct comparison of the correlation functions and, which is more enlightening, from the comparison of the thermodynamical data.[2] The PY II equation yields 0.40 for $\beta p/\rho$, when the "exact" result is 0.41 ± 0.01. For the state described here, the PY equation, as is well known, is no longer very good. This failure, not very apparent on $g(r)$, shows up very clearly in the thermodynamics. The value 0.51 is obtained for $\beta p/\rho$.

This defect is emphasized in Fig. 2, where the correlation function for $\rho=0.85$, $T=0.88$ is calculated both from molecular dynamics and PY equation. The exact result for $\beta p/\rho$ is 1.64. The PY compressibility factor is 3.18. The breakdown of the PY equation is obvious. As is well known, this equation gives a peak of $g(r)$ which is too high and too much to the left. This leads to an overestimation of the pressure as calculated from the virial theorem.

A table containing some of the values of the pair function obtained from the molecular dynamics computations is given in the Appendix.

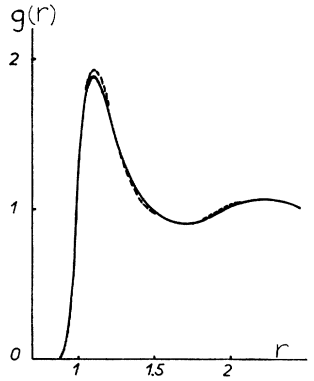

FIG. 1. The pair distribution function $g(r)$ as a function of r for $T=1.46$ and $\rho=0.4$. Solid line: results obtained both from molecular dynamics and from the PY II equation. Dashed line: PY equation.

[10] L. Verlet and D. Levesque, Physica (to be published).

III. EXTENSION OF THE MOLECULAR-DYNAMICS RESULTS

The pair function $g(r)$ has been obtained for $r<r_v$, using in the molecular-dynamics computation a Lennard-Jones potential cut at $r=r_v$. Let us label by MD the quantities directly obtained from the molecular-dynamics computation. We want to extend those results in two directions. Firstly, we want to take into account the tail of the potential: We shall show that the addition of this tail does not modify appreciably the short-range part of $g(r)$ (for $r<r_v$). We may anticipate that this is so in view of the fact that the thermodynamic results obtained with $r_v=3.3\sigma$ are consistent with those with $r_v=2.5\sigma$. Following a suggestion of Lebowitz, we can show it directly by considering the tail of the potential as a long-range perturbation and using the recently developed formalism[11] adapted to that problem. Let us define the long-range function

$$l(r)=-\beta V(r) \quad \text{for} \quad r>r_v \tag{5}$$

and its Fourier transform

$$\tilde{l}(k)=\rho\int e^{i\mathbf{k}\cdot\mathbf{r}}l(r)d\mathbf{r}. \tag{6}$$

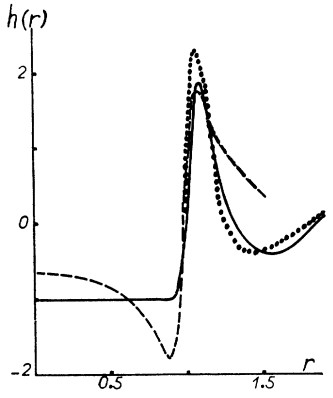

FIG. 2. Correlation function $h(r)=g(r)-1$ as a function of r for $T=0.88$ and $\rho=0.85$. ——: molecular dynamics. · · · · · : PY equation – – –: $h_1(r)$ as given by Eq. (31).

[11] M. Coppersmith and R. Brout, J. Chem. Phys. **130**, 2539 (1963); P. C. Hemmer, J. Math. Phys. **5**, 75 (1964); J. L. Lebowitz, G. Stell, and S. Baer, *ibid.* **6**, 1282 (1965).

Then, we shall sum the mixed ring composed of l bonds of $S_{MD}(k)$ bonds, where

$$S_{MD}(k)=\langle|\sum_{i=1}^{N} e^{i\mathbf{k}\cdot\mathbf{r}_i}|^2\rangle/N$$
$$=\tilde{h}(k)+1, \quad \text{for} \quad k>0. \tag{7}$$

$S_{MD}(k)$ is the structure factor for the problem with no long-range perturbation. It is easily seen that the variation $\delta g(r)$ of $g_{MD}(r)$ due the long-range tail is given by:

$$\delta g(r)=g_{MD}(r)L(r) \tag{8}$$

with

$$L(r)=\frac{1}{(2\pi)^3\rho}\int e^{i\mathbf{k}\cdot\mathbf{r}}\frac{\tilde{l}(k)d\mathbf{k}}{1-S_{MD}(k)\tilde{l}(k)}. \tag{9}$$

The calculation was performed in the case $T=1.05$, $\rho=0.75$. For $r>r_v=2.50$, we take $c(r)=0$, which is certainly, in the absence of a potential, an excellent approximation (the direction correlation for $r<r_v$ is already very weak). The Ornstein-Zernicke relation (1) and the definitions (8) and (9) are used in order to get $S_{MD}(k)$. The quantity $\delta g(r)$ is found to be everywhere smaller than 0.002. The inclusion of the static effect of the tail changes the thermodynamic functions by a negligible amount, as may be seen from Eqs. (10) and (11), which give respectively the change δp in the pressure and the change δU in the internal energy for the example we are considering.

$$\beta\delta p/\rho=\frac{-2\pi\rho}{3}\int_0^{r_v} r^3\frac{\partial V(r)}{\partial r}\delta g(r)dr$$
$$=-0.006 \tag{10}$$

$$\delta U=2\pi\rho\int_0^{r_v} r^2V(r)\delta g(r)dr$$
$$=0.005. \tag{11}$$

In our computations, the statistical error in $\beta p/\rho$ and in the internal energy is of the order of 0.01. We thus see that within the claimed accuracy we can neglect the influence of the tail of the potential on the computed correlation function.

The second and more tricky point has to do with the extension of our results to all values of r. This is necessary inasmuch as we want to reach $\tilde{h}(k)$, and it is unadvisable to Fourier-transform a truncated $h(r)$.

Our extrapolation technique has been explained in the Introduction: We choose for $c(r)$, $r>r_c$, the expression given by the PY Eq. (2). We make the cutoff at one of the zeros of $h(r)$ so as to ensure the continuity of the direct correlation function, as may be seen from the Ornstein-Zernicke relation (1). The fitness of our extrapolation can be appreciated from Table I, where in the high-density cases one compares $\beta p/\rho$, the inverse compressibility, and the height of the first peak of $\tilde{h}(k)$ for various values of the cutoff. It is seen that, when the PY equation is used for the continuation, it is only necessary, even at high density and low temperature, to include the first peak of the "exact" $g(r)$. We also try replacing $c(r)$ by $f(r)$ immediately after the first peak of $g(r)$. The results are not excellent, but clearly much better than those obtained when the PY equation is used for all values of r.

Also, we can compare, when $r_c<r_v$, the extrapolated $g(r)$ with the exact one: The differences are small. They are smaller than the statistical errors in $g(r)$. We see again that there is no reason to prefer the molecular-dynamics results to the extrapolated ones for the correlation function after its first peak.

The determination of the inverse compressibility is made through

$$\beta\partial p/\partial\rho=1/[1+\tilde{h}(0)]. \tag{12}$$

Although the results thus obtained are compatible with the equation of state, they are not precise enough to be useful: The uncertainty on the inverse compressibility is of the order of 10%.

IV. DIRECT CORRELATION FUNCTION AND THE POTENTIAL-INVERSION PROBLEM

Examples of the direct correlation function calculated as said in the last section are shown in Figs. 3 and 4. It is seen that $c(r)$ behaves very much as an intuitive

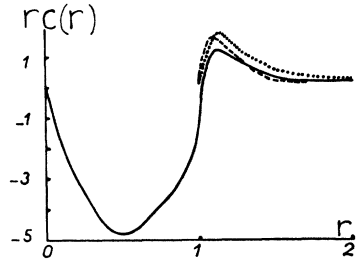

FIG. 3. Direct correlation function $c(r)$ multiplied by r as a function of the distance for $T=1.05$ and $\rho=0.75$. ——: $c(r)$ obtained from molecular dynamics through the extension procedure described by Eqs. (1) and (2) with $r_c=2.32$. · · · · · : $c(r)=f(r)$, when $r>1$. – – –: $c(r)=g_{MD}(r)/(e^{\beta V(r)}-1)$, where $g_{MD}(r)$ is the pair distribution function obtained from molecular dynamics.

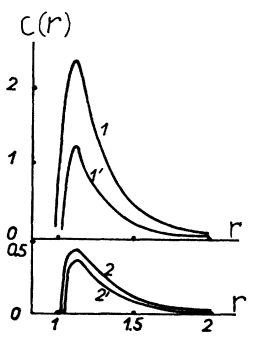

FIG. 4. Two examples of direct correlation functions [Eqs. (1) and (2) were used, with $r_c=2.32$]. (1) $T=0.827$, $\rho=0.75$. Curve (1): $f(r)$. Curve (1'): $c(r)$. (2) $T=2.845$, $\rho=0.75$. Curve (2): $f(r)$. Curve (2'): $c(r)$.

guess would indicate. For $r<\sigma$, a large dip in $rc(r)$ represents the exclusion due to the hard core, as in the Wertheim-Thiele hard-sphere gas. When r approaches σ there is a sharp rise, and $c(r)$ vanishes, within 2 or 3%, at the same point as the potential. For large r, $c(r)$ has the same aspect as $f(r)$. It is somewhat smaller, and more so at lower temperature. In Fig. 3, we have also plotted the direct correlation function obtained from the PY relation (2). We see that it is peaked too far to the left.

The situation would be worsened if the PY equation were really solved, because that equation leads to a pair function which has a peak too high and too far to the left [see Fig. (2)].

Once $c(r)$ and $g(r)$ are known, the validity of the PY Eq. (2) can be tested by using it to calculate a potential which should be strictly equal to the initial Lennard-Jones potential if that equation were exact. Thus one can know when the PY equation can be used to obtain the potential using experimental data.

For densities around critical, the PY equation may be safely used to get the potential back from the computed correlation function: For instance, at the density $\rho=0.4$, and for $T=1.33$, the calculated potential is less deep than the Lennard-Jones potential by 1% in the region of the bowl of the potential. It is deeper, on the other hand, for larger values of r ($1.2<r<1.60$), but the error is never larger than 4%. The error rises rapidly with the density, as can be seen in Fig. 5: The PY equation for dense liquids cannot lead to a quantitatively reliable determination of the effective two-body interaction. Attempts were made by Mikolaj and Pings[7] to obtain the effective two-body interaction between argon atoms from the x-ray scattering intensity measured in the vicinity of the critical point: For $\rho=0.165$ these authors obtain a potential which resembles the Lennard-Jones one. The potential obtained

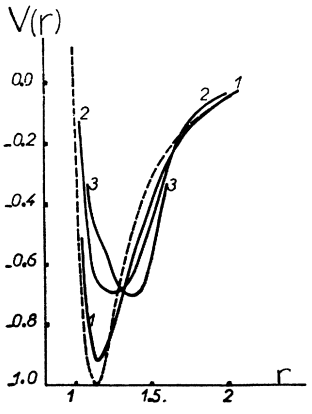

FIG. 5. Potential obtained from the correlation function, using the PY Eq. (2): Curve (1): $T=1.328$, $\rho=0.5426$. Curve (2): $T=1.05$, $\rho=0.75$. Curve (3): $T=1.127$, $\rho=0.85$. The Lennard-Jones potential, which should be obtained if the PY equation were exact, is represented by the dashed curve.

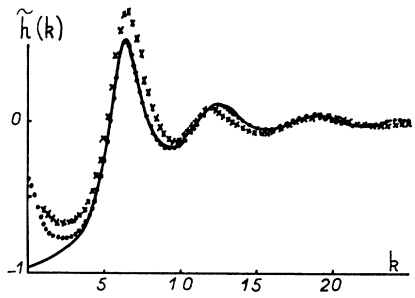

FIG. 6. $\tilde{h}(k)$ as a function of k. Dots: Results from molecular dynamics for $T=1.326$, $\rho=0.5426$. Solid line: hard-sphere model, with the hard-sphere diameter $a=1.0$ and the hard-sphere density $\hat{\rho}=0.57$. Crosses: x-ray experiment (Ref. 7) at the same density and $T=1.28$.

rises as a whole by 15% when the density increases to 0.316, and again by 15% when the density 0.46 is reached. One could try to explain these results by postulating an effective interaction between the argon atoms that depends strongly on the density. The equation of state obtained from the Lennard-Jones potential is so good[2] that such a strong state dependence may seem unlikely. For reasons that will become apparent in Sec. VIII, we believe that it is very important that the experiments reproduce carefully the oscillations of $\tilde{h}(k)$ for large values of k. Any error in the oscillation period will always lead to an underestimation of the maximum of $g(r)$, and thus, of the derived interaction. Typical experimental data[7] are compared with the results of molecular dynamics on Fig. 6: They do not agree very well.

V. ON THE MAIN PEAK OF $\tilde{h}(k)$

Once $c(r)$ is known, $\tilde{h}(k)$ can be calculated from $\tilde{c}(k)$ and the Ornstein-Zernicke relation (1), Fourier-transformed as

$$\tilde{h}(k)=\tilde{c}(k)/[1-\tilde{c}(k)]. \tag{13}$$

Figures 6–8 show examples of the results so obtained, together with a comparison with experiment. Equation (13) tells us that the first maximum of $\tilde{h}(k)$ located

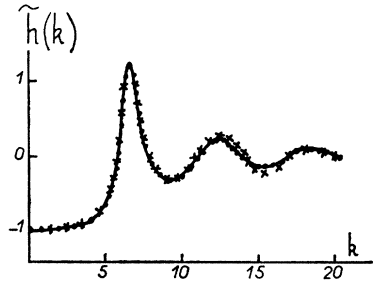

FIG. 7. $\tilde{h}(k)$ as a function of k. Dots: results from molecular dynamics for $T=0.827$, $\rho=0.75$. Solid line: hard-sphere model, with $a=1.03$, $\hat{\rho}=0.817$. Crosses: neutron experiment (Ref. 14) on krypton. $\rho=0.77$, $T=0.77$.

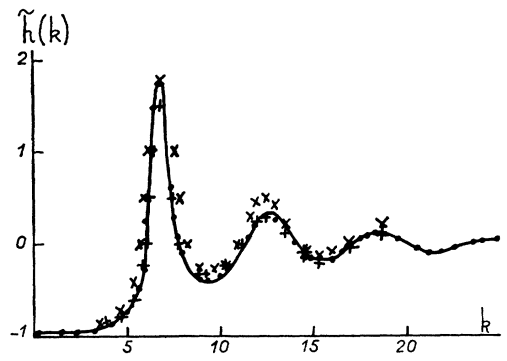

FIG. 8. $\tilde{h}(k)$ as a function of k. Dots: Results from molecular dynamics for $T=0.723$, $\rho=0.844$. Solid line: hard-sphere model with $a=1.026$, $\hat{\rho}=0.91$. +: neutron experiment on argon at the same density and $T=0.7$ (Ref. c of Fig. 10). ×: x-ray experiment on argon at the same density and $T=0.70$ (Ref. b of Fig. 10).

at $k=k_0$ is also a maximum of $\tilde{c}(k)$. How is such a maximum produced? To see this qualitatively, let us consider Fig. 3, which shows a typical direct correlation function [$rc(r)$, to be precise], for $T=1.05$, $\rho=0.75$. We remark that $c(r)$ changes its sign in the neighborhood of $r=\sigma$ and is varying very rapidly in that region. If the PY Eq. (2) were valid, $c(r)$ would vanish strictly at $r=\sigma$, and the steepness of its variation would be simply related to that of the potential. Generally, we can write[12]

$$c(r)=g(r)(e^{\beta V(r)}-1)+\Phi(r) \tag{14}$$

where $\Phi(r)$ is the correction, which is given, in first approximation, by the PY II equation. The terms composing $\Phi(r)$ are expected to vary rather smoothly with r. Whenever that correction term is not very large, we expect $c(r)$ to retain the characteristics yielded by the PY equation. Figures (3) and (4) show that this is indeed the case. We might add that, if nonadditive parts of the many-body forces are present, they should produce an effective additional two-body interaction relatively smooth at $r=\sigma$, and the zero of $c(r)$ should not be changed. The sharpness of $c(r)$ around the zero of the potential has the following consequence: $\tilde{c}(k)$ will be obtained by multiplying $rc(r)$ by $4\pi\rho(\sin kr)/k$ and integrating over r. Let us consider a value of k such that there are approximately two arches of the sine for $r<\sigma$. The first arch, combined with $rc(r)$, will bring a negative contribution. The next arch gives a positive contribution. If the third arch starts a little before $r=\sigma$, it gives first a negative contribution and then, as a result of the positive part of $c(r)$, a positive one. As a whole, a compromise is reached, so that the second arch gives the maximum possible contribution, with due attention to the fact that too much should not be lost at the beginning of the third arch. Clearly, this is realized for $k_0=2\pi/r_0$, where r_0 is presumably a little less than σ, and should depend very little on the state. The results, of little interest, for $\rho<0.2$ have been obtained through the PY equation. As expected, r_0 is of the order of σ. The qualitative explanation of the temperature variation for a given density goes as follows: When the temperature is low, the positive part of $c(r)$, which behaves very much like $f(r)$, is large. Then the third arch of the sine tries to use this chance as much as possible: r_0 is equal to σ or a little more. If the temperature is large, on the other hand, the negative part of $c(r)$, similar to that of a hard core, is the most important factor and r_0 decreases so as to maximize the second arch. As a whole the effect of the temperature is very small, as may be seen from Fig. 9, where r_0 has been plotted for several high-density isochores. The variation of r_0 with the density is more important. It resembles that of a hard-core gas, as may be seen from Fig. 10. There, one compares r_0 as a function of the density in the case of the Lennard-Jones potential for the temperature $T=1.35$ with the same quantity for a hard-sphere gas of diameter σ. The hard-sphere-gas curve is drawn using the Thiele-Wertheim solution.[5] The "exact" results obtained from a Monte-Carlo computation appear to differ very little.[13] On the same plot are shown the results of x-ray and neutron scattering experiments on argon and krypton. The agreement between calculation and experiment (and between the experiments) is much better at high than at low density. It is to be noted, however, that the results from the neutron experiment of Clayton and Heaton[14] agree very well with the predicted curve for r_0.

VI. ON THE ASYMPTOTIC FORM OF $h(r)$

In this section we shall try to understand, on physical grounds, the behavior of $h(r)$ for large values of r. For high values of the density, the oscillations of the correlation function constitute its most striking feature,

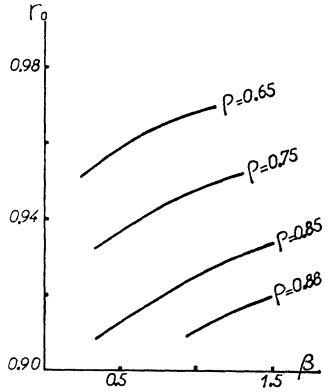

FIG. 9. $r_0=2\pi/k_0$, where k_0 is the location of the first peak of $\tilde{h}(k)$ as a function of $\beta=1/kT$ for the isochores $\rho=0.88$, $\rho=0.85$, $\rho=0.75$, $\rho=0.65$.

[12] G. Stell, in *The Equilibrium Theory of Classical Fluids*, edited by H. L. Frisch and J. L. Lebowitz (W. A. Benjamin, Inc., New York, 1964).

[13] D. Schiff and L. Verlet, Phys. Rev. **160**, 208 (1967).

[14] G. T. Clayton and L. Heaton, Phys. Rev. **121**, 649 (1961).

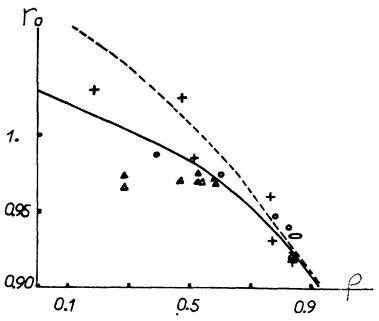

FIG. 10. r_0 as a function of ρ for the Lennard-Jones potential at the temperature $T=1.35$ (solid line), and for the hard-sphere gas of diameter 1 (dotted line). Experimental data: ○: neutrons on krypton (Ref. 14). △: x rays on argon (Ref. 7). +: x rays on argon [A. Eisenstein and N. S. Gingrich, Phys. Rev. **62**, 261 (1942)]. (ellipse): x rays on argon [N. S. Gingrich and C. W. Thompson, J. Chem. Phys. **36**, 2398 (1962)]. □: neutrons on argon [D. G. Henshaw, Phys. Rev. **105**, 976 (1956)]. ×: neutrons on argon [D. A. Dasannachaiya and K. R. Rao, Phys. Rev. **137**, A417 (1965)]. The reduction parameters are, for krypton: [J. A. Beattie, R. J. Barriault, and J. S. Brierly, J. Chem. Phys. **19**, 1222 (1951)]. $\sigma=4.064$ Å, $\epsilon/k=224.5°$ and, for argon: [A. Michels, H. Wijker, and H. K. Wijker, Physica **15**, 627 (1949)]. $\sigma=3.405$ Å, $\epsilon/k=119.8°$.

and we shall attempt to characterize them as due to a hard-core effect.

It will help us, we believe, to understand the case of the Lennard-Jones potential if we examine first two simpler and less realistic examples.

(1) Let us suppose, first, that $c(r)$ is of short range a and that the inverse compressibility is not very large. An illustrative example of that kind of situation is presented by the solution of the PY equation for the hard-sphere+square-well potential.[15] Let us assume that for large values of r

$$h(r)=A_\lambda(e^{-\lambda r}/r)+A_\mu(e^{-\mu r}/r)\sin k_0 r. \tag{15}$$

We shall insert this form in the Ornstein-Zernicke relation (1), which reads, when r is outside the range of the direct correlation function:

$$h(r)=\frac{2\pi\rho}{r}\int_0^\infty c(s)sds\int_{|r-s|}^{r+s}h(t)tdt. \tag{16}$$

Then it is readily seen that (15) is compatible with the Ornstein-Zernicke relation if the Fourier transforms of the direct correlation function obey the conditions:

$$\tilde{c}(k_0+i\mu)=1 \tag{17}$$

$$\tilde{c}(i\lambda)=1. \tag{18}$$

Let us introduce the Yvon generalized response function[16]

$$\delta\rho_k/-\beta\delta U_k=1+\tilde{h}(k)=1/[1-\tilde{c}(k)], \tag{19}$$

where U_k is the k Fourier component of an external potential $U(r)$. The conditions (17) and (18) are satisfied if there are poles in (19) for the complex wave numbers $k_0+i\mu$ and $i\lambda$. In particular a particle placed at the origin provokes in the medium the response described by (15).

Let us remark that $\tilde{c}(0)=1$ would mean that there is a real pole at the origin and that $1/r$ is the asymptotic solution. We know that when the inverse compressibility is zero the singularity is no longer a pole and that $c(r)$ does not stay short-ranged. $\tilde{c}(k_0)=1$ would indicate the possibility of sustaining an undamped sinusoidal solution. Such a solution does exist in the PY approximation for the lattice gas with repulsive interaction, but it can be shown that this solution does not represent a physical state of the system.[17] The condition (19) can be expressed as

$$4\pi\rho\int_0^\infty c(s)s^2ds\frac{\sinh(\lambda s)}{\lambda s}=1; \tag{20}$$

expanding in powers of λ, the Ornstein-Zernicke relation is recovered:

$$\lambda^2=6\left(1-\rho\int c(r)d\mathbf{r}\right)\Big/\rho\int r^2c(r)d\mathbf{r}. \tag{21}$$

In many cases (20) or (21) are not very useful, as they enhance the tail of $c(r)$, which may be an inconvenience in those cases where $c(r)$ is not strictly short-ranged. In the same way, we can write (17) as two coupled equations giving μ and k_0.

If around $k=0$, we can write:

$$\tilde{h}(k)\simeq 4\pi A_\lambda\rho/(k^2+\lambda^2) \tag{22}$$

that is, if the pole $k=i\lambda$ clearly dominates, then $\tilde{c}(k)$ is also of the Lorentz form:

$$\tilde{c}(k)=4\pi A_\lambda\rho/(k^2+\lambda^2+4\pi A_\lambda). \tag{23}$$

The condition $\tilde{c}(i\lambda)=1$ is automatically satisfied, and λ can be fixed by calculating the half-width of $\tilde{h}(k)$.

In the same way, if the pole $k=k_0+i\mu$ clearly dominates,

$$\tilde{h}(k)\simeq\frac{2\pi A_\mu\rho\mu}{k_0[(k-k_0)^2+\mu^2]} \tag{24}$$

and (17) is satisfied. k_0 corresponds to the maximum of $\tilde{c}(k)$ and μ can be determined through half-width arguments.

If the density is not too high, the situation still corresponds qualitatively to the above description. If we choose, for instance, a density not far from critical, say $\rho=0.3$, $T=1.3$, then the description by the PY equation is still fairly good: the correlation function is shown in Fig. 11, and behaves qualitatively as described by (15). The main maximum k_0 of $\tilde{c}(k)$ is at $k_0=6.1$. The oscillating part has the same periodicity as $\sin k_0 r$. If we try to fit λ and μ directly, we see that the predictions of ex-

[15] D. Levesque, Physica **32**, 1985 (1966).

[16] J. Yvon, Nuovo Cimento Suppl. **9**, 144 (1958).

[17] B. Jancovici, Physica **31**, 1017 (1965).

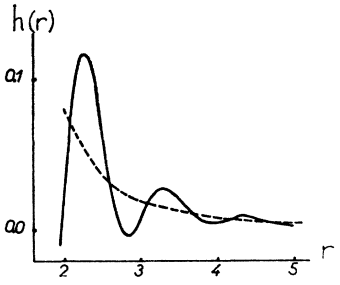

FIG. 11. Correlation function $h(r)$ for the hard-sphere+square-well model obtained from the PY equation, for $T=1.3$, $\rho=0.3$. (This corresponds to a low inverse compressibility). $h(r)$ oscillates around the dashed curve, as shown by Eq. (15).

ponential damping are not very well verified: roughly, we obtain $\lambda=0.7$, $\mu=1.3$. Using the half-width of the peaks of $\tilde{h}(k)$ around $k=0$ and $k=k_0$, we find $\lambda=0.5$, $\mu=0.7$: it is normal that there should be more damping than indicated by a forced single-pole description. Evidently, (15) would be better if we went closer to the transition line (the pole $k=i\lambda$ would become more dominant), especially if we increased the density simultaneously.

(2) Let us take now an example where, again, $c(r)$ is of range a, but where now $\partial p/\partial\rho$ is large. We would like to express that condition by writing for $k\sim 0$,

$$\tilde{c}(k)=-4\pi B\rho/(k^2+\nu^2). \tag{25}$$

This leads to a term $e^{-\nu r}/r$ in $c(r)$. The function $c(r)$ stays essentially short-ranged, however, if $\nu\gg 1/a$.

On the other hand, we suppose that $h(r)$ has still an asymptotic behavior of the dampled oscillating form

$$h_a(r)=A_\mu(e^{-\mu r}/r)\sin k_0 r. \tag{26}$$

It is not difficult to see that for large r, Eqs. (25) and (26) are compatible with the Ornstein-Zernicke relation if both (17) and the condition

$$\tilde{h}(i\nu)=-1 \tag{27}$$

are satisfied.

Referring again to the Yvon response function (19), the first condition expresses the fact that the medium responds to a perturbation of wave number k_0; the condition (27), on the other hand, describes the stability of the medium against long-wavelength perturbations.

We use again as an example the PY equation, this time for hard spheres[5] at high density: $\eta=\pi\rho/6=0.35$. Around $k=0$, $\tilde{c}(k)$ is entirely dominated by the nearby pole at $k=0$. The effect of the pole at $k=k_0$ is clearly negligible. Fitting $\tilde{c}(k)$ with Eq. (25), we find $4\pi B\rho=115$, $\nu=2.75$.

Then, we can say that around $k=k_0$, $\tilde{h}(k)$ is given by

$$\tilde{h}(k)=\frac{-4\pi B\rho}{k^2+\nu^2+4\pi B\rho}+\frac{2\pi\mu A_\mu\rho}{k_0}\frac{1}{(k-k_0)^2+\mu^2}. \tag{28}$$

Using the values of B and ν just determined, we can extract from $\tilde{h}(k)$ the part due to the pole at the origin. We thus get $A_\mu=2.5$, $\mu=1.15$. The direct fit of $h(r)$ by (26) leads to $A_\mu=2.6\pm 0.25$, $\mu=1.16\pm 0.03$; the dominant pole representation for the asymptotic part of $h(r)$ is thus seen to be excellent.

(3) The case of the Lennard-Jones potential. The striking fact is that, here again, $h(r)$ behaves as $\sin k_0 r$ at high density, where $k_0=2\pi/r_0$ is the position of the first peak of $\tilde{h}(k)$ as discussed before. It is therefore clear that the oscillations of $h(r)$ are a consequence of the sharp repulsion of the potential. The accuracy with which this sine rule holds is illustrated by the first three lines of Table II. These give, for three high-density cases, the values of r_0 obtained from $\tilde{h}(k)$ and the values r_{0i} obtained by fitting the successive zeros of $h(r)$ with $\sin(2\pi r/r_{0i})$ starting from the third zero, that is, excluding such zeroes as belong to the first peak of the correlation function. The fourth line shows that the oscillations do not have the same regularity when $\partial p/\partial\rho$ is small. We cannot go further and apply the analysis given in the preceding example to the case of the Lennard-Jones potential, because $c(r)$ is no longer strictly short-ranged. Actually the asymptotic form (26) is not valid in the present case; the decay of $h(r)$ is only very poorly approximated by that formula, with μ roughly of the order of σ. The following point should be stressed: at low density $h(r)$ behaves as $f(r)$. On the other hand, we have at high density oscillations of the damped sine type. To obtain such a result one needs a strong screening of the potential. In order to understand how such a screening operates, we remember that the correlation function, according to (19), is to be seen as the response of the medium to a test particle at the origin. The tail of the potential can be considered as a long-wavelength perturbation. At higher density $\partial p/\partial\rho$ is large, and this corresponds to a high stability of the medium against those perturbations: The potential is very effectively screened out. When $\partial p/\partial\rho$ is small, on the other hand, the decay of the correlation is complicated; it results from the combination of the little-screened long-range part of the potential and the many-body effects described in the preceding section: the oscillations can no longer be described by a sine, as may be seen from the last line of Table II. The analysis made by Enderby, Gaskell, and March[18] makes the above con-

TABLE II. Values of $r_{0i}=2R_i/(1+i)$ where R_i is the position of the ith zero of $h(r)$ (columns 3 to 7). In column 8 is given $r_0=2\pi/k_0$ where k_0 is the location of the main peak of $\tilde{h}(k)$. The inverse compressibility is given in column 9.

ρ	T	r_{03}	r_{04}	r_{05}	r_{06}	r_{07}	r_0	$\beta\partial p/\partial\rho$
0.85	2.205	0.915	0.905	0.915	0.915	0.915	0.912	20
0.75	0.827	0.95	0.945	0.95	0.95	0.955	0.951	13
0.65	0.90	0.965	0.955	0.965	0.97	0.97	0.963	3
0.45	1.522	0.99	1.04	0.995	1.03	0.99	0.99	1.2

[18] J. E. Enderby, T. Gaskell and N. H. March, Proc. Phys. Soc. 85, 217 (1965).

TABLE III. Values of r_i such that $k_i r_i = (1+i)\pi$, where k_i is the position of the ith zero of $\tilde{h}(k)$. The first line corresponds to x-ray experiments[a] and should be compared with the second line (molecular dynamics). Similarly the neutron data[b] of line 3 are to be compared with the molecular-dynamics results of line 4.

	T	ρ	r_3	r_4	r_5	r_6	r_7	r_8
x-ray[a]	1.28	0.5426	1.11	0.94	1.10	1.05	0.985	0.955
MD	1.326	0.5426	1.10	1.10	1.09	1.08	1.07	1.06
neutron[b]	0.77	0.77	1.13	1.12	1.10	1.10	1.10	1.07
MD	0.827	0.75	1.13	1.13	1.11	1.10	1.09	1.08

[a] Reference 7.
[b] Reference 14.

siderations more quantitative: In a diagrammatic expansion, it is easily seen[12] that $c(r)$ contains, in addition to $f(r)$, an infinity of diagrams with no articulation points. Given that $f(r)$ behaves for large r as $-4\epsilon\beta(\sigma/r)^6$, each of those terms goes to zero faster than $1/r^6$. If the same can be said of the sum of all those terms, the asymptotic behavior of $c(r)$ is known. Simple considerations on the Fourier transforms lead, with the help of the Ornstein-Zernicke formula (1), to the conclusion that for large values of r, the function $h(r)$ behaves as:

$$h(r)\sim f(r)/(\beta\partial p/\partial\rho)^2. \tag{29}$$

Thus, at high density, where the inverse compressibility is large, the tail of the potential is almost suppressed, and may be seen only at very large distances, where the many-body effects have died out. Theoretically, the asymptotic form, for very large r, is probably given by (29). Practically the many-body effects dominate the observable range, and $h(r)$ is of the form $\varphi(r)\sin k_0 r$, where $\varphi(r)$ is some damping function that we have not been able to write down explicitly.

VII. ASYMPTOTIC BEHAVIOR OF $\tilde{h}(k)$

We shall try, analogously to what has been done for the large-r behavior of $h(r)$, to relate the asymptotic form of $\tilde{h}(k)$ to the first peak of $g(r)$. The important components in the Fourier transform of the correlation function will correspond to the location r_m of its maximum and to the steeply varying portion in the neighborhood of $r\simeq\sigma$.[19] To illustrate that point, we show in Table III for two cases the values r_i of r such that

$$k_i r_i = (1+i)\pi,$$

where k_i is the position of the ith zero of $\tilde{h}(k)$. We see that the first r_i considered is equal to r_m and that the successive zeros lead to lower values of r_i, as the rising part of $g(r)$ is explored in the Fourier transform. In Table III, we compare the values of r_i of one of Pings's experiments[7] ($T=1.28$, $\rho=0.5426$) with the result of a molecular-dynamics computation ($T=1.326$, $\rho=0.5426$). We do the same for one of Clayton and Heaton's[14] experiments ($T=0.77$, $\rho=0.77$) and compare it with our nearest "experiments" ($T=0.827$, $\rho=0.75$). We immediately see the striking contrast between the regularity of the neutron data and the more erratic character of the x-ray data. The complete comparison of $\tilde{h}(k)$ in both cases is shown in Figs. 6 and 7.

More precisely, we find that our results for $\tilde{h}(k)$ can be fitted for large k values by the form

$$\tilde{h}_a(k)=C\cos kr_w\exp(-\alpha k)/k \tag{30}$$

r_w and α are represented as functions of β for several isochores in Figs. 12 and 13 respectively. It has been

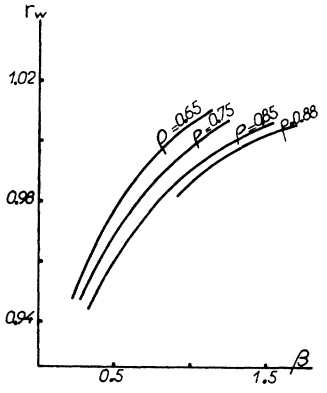

FIG. 12. r_w of formula (30) as a function of β for the isochores $\rho=0.88$, $\rho=0.85$, $\rho=0.75$, and $\rho=0.65$.

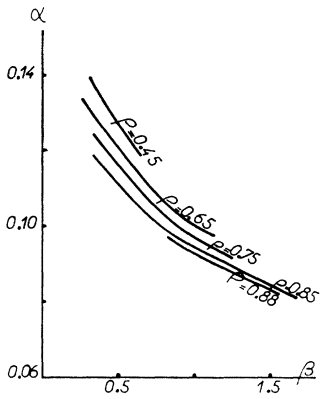

FIG. 13. α of formula (30) as a function of β for the isochores $\rho=0.88$, $\rho=0.85$, $\rho=0.75$, $\rho=0.65$, and $\rho=0.45$.

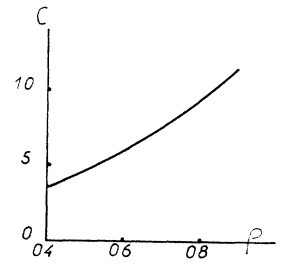

FIG. 14. C of formula (30) as a function of ρ.

[19] R. Kaplow and S. L. Strong (private communication).

found sufficient with those values of r_w and α to take C as depending only on ρ (Fig. 14). The exponential decay in (30) is quite well verified. The oscillations in $\tilde{h}(k)$ are reproduced by (30) to a fair degree of accuracy: The error in the positions for the first five zeros of $\tilde{h}(k)$ after those belonging to the first peak is less than 0.1 in reduced units. A slightly better fit would be obtained by introducing a phase shift in (30). Let us now represent $h(r)$ in the neighborhood of its first peak by

$$h_1(r)=\frac{C'}{4\pi^2\rho r}\left[\frac{r-r_w'}{\alpha^2+(r-r_w')^2}+\frac{r+r_w'}{\alpha^2+(r+r_w')^2}\right]. \quad (31)$$

When r_w' and C' are equal to r_w and C respectively, (31) is precisely the Fourier transform of (30). It turns out that they are not exactly equal, but very nearly so. r_w' is smaller than r_w roughly by 0.005, and C' is equal to C within 10% in general. Although such an excellent agreement is probably coincidental in part, it indicates the close connection between the oscillations of $\tilde{h}(k)$ and the peak of $h(r)$. The approximate representation $h_1(r)$ of the correlation function given by (31) is shown on Fig. 2 in one of the high-density cases ($\rho=0.85$, $T=0.88$). $h(r)$ vanishes approximately for

$$r\simeq r_w'+\alpha^2/2r_w'$$

where the second term is very small; above this value $h(r)$ rises linearly and then bends over to reach a maximum at $r_m\simeq r_w'+\alpha$. Lastly, it is easy to see that the following relation holds between the maximum of the correlation function given by (31) and the slope of its rising part:

$$h_1(r_m)/r_w'dh_1(r)/dr]_{r=r_w'}\simeq\alpha/2r_m.$$

This relation holds also, to a good approximation, for the exact correlation functions, as may be seen from the data presented in the Appendix.

VIII. HARD-SPHERE MODEL FOR THE LENNARD-JONES POTENTIAL

In the preceding sections, we have emphasized the importance of the repulsive part of the potential and the likeness of its effects to those of an infinitely hard core. Before proceeding further we shall briefly summarize the conclusions which have been reached in the preceding sections. We have seen in Sec. IV that the direct correlation function for the Lennard-Jones potential presents near the origin a large negative arch characteristic of the repulsive region of the potential, and a steeply rising part in the region where the potential varies rapidly around zero. This behavior very much resembles that of a rigid-sphere gas. The shape of the direct correlation function inside the repulsive region of the potential fixes almost completely the position of the main peak of $\tilde{h}(k)$ at a value which at high density is practically the same as that for a hard-sphere gas of the same density and of diameter σ. This peak of $\tilde{h}(k)$ is responsible for the oscillations of $h(r)$ for large values of r, and the position k_0 of the peak determines the period $r_0=2\pi/k_0$ of these oscillations. Lastly, we have seen in Sec. VIII that the oscillations of $\tilde{h}(k)$ for large values of k are closely related to the steeply rising part of the correlation function, which is due to the rapid change of the potential in the region $r\simeq\sigma$. More precisely, $\tilde{h}(k)$ oscillates as $\cos kr_w$, where r_w is practically equal to the value of r at the first zero of the correlation function $h(r)$.

Given those remarks, it is very tempting to generalize the hard-sphere model used by Ashcroft and Lekner[9] in their study of the correlation functions of liquid metals: we shall try to fit $\tilde{h}(k)$ for the Lennard-Jones potential with that corresponding to a hard-sphere gas. The density of the equivalent hard-sphere gas will be chosen in such a way that the heights of the first peaks of the two structure factors coincide. The height $\tilde{h}(k_0)$ is shown on Fig. 15 in the case of the Lennard-Jones fluid for several values of the density ρ as a function of the inverse temperature β. On those isochores is shown also the value of $\tilde{h}(k_0)$ obtained from the Wertheim-Thiele solution corresponding to a hard-sphere gas of diameter σ and of density $\hat{\rho}=\rho$. If we follow Ashcroft and Lekner and take the diameter of the equivalent hard-sphere gas equal to σ, and if we fit its density $\hat{\rho}$ by requiring the coincidence of the heights of the first peaks of $\tilde{h}(k)$, we obtain for each isochore of the Lennard-Jones potential a curve giving $\hat{\rho}$ as a function of β, as shown on Fig. 16. The diameter of the hard sphere will not be taken equal to σ, but to a slightly different value a, chosen in such a way that the zeros of $\tilde{h}(k)$ away from the main peak coincide with those of the model $\tilde{h}(k)$. Remembering that the asymptotic form of the Wertheim-Thiele solution of the hard-sphere problem behaves as $(\cos ka)/k^2$,

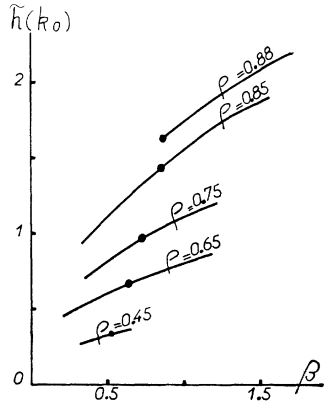

FIG. 15. Height of the first peak of $\tilde{h}(k)$ as a function of the inverse temperature β for several isochores. The dots indicate the height of the first peak of the hard-sphere model of diameter σ at the same density.

we would be tempted, in view of (30), to take a equal to r_w. That asymptotic form, however, is reached only for very large values of k. We thus prefer to fit a directly in such a way that the first zeroes after the main peak of both $\tilde{h}(k)$'s coincide. The values of a resulting from such a fit are shown for several isochores, as a function of the temperature, on Fig. 17. It is seen that, as was the case for r_w, a decreases when the temperature increases, as expected intuitively. We see from Figs. 6–8 that such a model, which is only fair at the lowest density considered (Fig. 6), becomes excellent for very high values of the density. It should be said, however, that the decay at very large k is not at all the same for the two cases: This is not apparent on the figures, but may be seen from the data, and is a reflection of the fact that the peaks of $g(r)$ are very different for hard spheres and Lennard-Jones molecules.

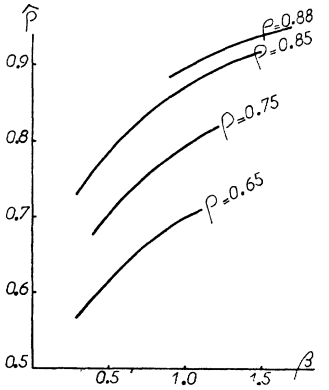

FIG. 16. Density $\hat{\rho}$ of the hard-sphere model of diameter σ fitting the height of the first peak of $\tilde{h}(k)$ to that of a Lennard-Jones fluid as a function of the inverse temperature β for several values of the density.

If the model were really consistent, the actual density ρ' of the hard-sphere gas of diameter a, i.e. $\hat{\rho}/a^3$, would be equal to ρ. This is indeed so at high density. For instance, for the twelve temperatures considered on the isochore $\rho=0.85$, all values of ρ' obtained are situated between 0.84 and 0.85. Therefore, if we write $a=(\hat{\rho}/\rho)^{1/3}$, the error is very small. At lower density this approximation is not so good. For instance, for $\rho=0.5426$, $T=1.328$, one gets $\hat{\rho}=0.572$ and $\rho'=0.56$: The error in a reaches 1%.

It is easily seen, using Figs. 9, 10, 16, and 17, that at high density, the position of the first peak of the molecular-dynamics $\tilde{h}(k)$'s and that yielded by the hard-sphere model coincide, to a good accuracy. From this, it results (see Sec. VI) that the oscillations of $h(r)$ will be correctly reproduced by the model.

A last remark concerns the low-k behavior. For high densities, both the hard-sphere gas and the Lennard-

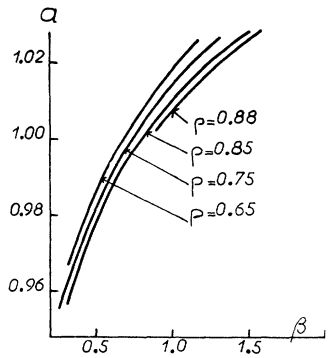

FIG. 17. Diameter a of the model hard-sphere gas as a function of the inverse temperature β of the Lennard-Jones fluid, for several isochores.

Jones fluid are very incompressible, and the structure factor scoincide fairly well for low values of k (Figs. 7 and 8). If, on the other hand, the density is relatively low and the temperature around critical, the hard-sphere gas is much more incompressible than the Lennard-Jones fluid, and the structure factor yielded by the model differs radically from the exact one (Fig. 6). We realize again that, because of the high inverse compressibility, this model is more appropriate at high density, where the potential effects are screened out.

IX. CONCLUSION

In this paper, we have presented an analysis of the correlation functions obtained from molecular dynamics in the case of the Lennard-Jones potential. It has been made clear that most of the structure of the correlation functions at high density is due to the geometrical effects produced by the existence of a strong repulsion in the potential. It has been shown that these effects can be displayed by the Wertheim-Thiele approximate solution of the hard-sphere problem, and that the diameter a of the hard spheres is the only parameter of the theory. In a forthcoming paper[13] we shall show that these results are not spoiled if the exact (numerical) solution of the hard-sphere problem is used, and how the Kirkwood-Alder transition of the model hard-sphere gas is related to the actual liquid-solid transition.

APPENDIX

In this Appendix we give a table of the values of some of the pair functions $g(r)$ which have been computed and used in the present study (Table IV). For $r\leq 2.4$, the results are obtained directly through the molecular-dynamics computation. The results for larger values of the distance are obtained with the help of the extrapolation procedure described in the Introduction. It may be recalled that, for high densities, $g(r)$ is equal to unity when $\sin(2\pi r/r_0)$ vanishes. r_0 is given in Figs. 9 and 10.

TABLE IV. The pair function $g(r)$ for several values of the density ρ and the temperature T. The units are the usual reduced units with $\sigma = \epsilon/k = 1$.

ρ / T / r	0.880 1.095	0.880 0.936	0.880 0.591	0.850 2.888	0.850 2.202	0.850 1.273	0.850 1.127	0.850 0.880
0.84	0.000	0.000	0.000	0.007	0.001	0.000	0.000	0.000
0.88	0.001	0.000	0.000	0.145	0.060	0.004	0.002	0.003
0.92	0.086	0.048	0.003	0.716	0.490	0.135	0.085	0.030
0.96	0.688	0.520	0.169	1.545	1.310	0.799	0.610	0.412
1.00	1.871	1.691	1.128	2.093	2.076	1.846	1.750	1.511
1.04	2.701	2.682	2.592	2.210	2.350	2.508	2.560	2.546
1.08	2.785	2.899	3.279	2.069	2.228	2.587	2.710	2.871
1.12	2.453	2.584	3.032	1.834	1.973	2.309	2.413	2.594
1.16	2.003	2.111	2.440	1.586	1.699	1.944	2.009	2.151
1.20	1.596	1.682	1.864	1.372	1.438	1.597	1.643	1.744
1.24	1.286	1.337	1.401	1.196	1.223	1.323	1.349	1.386
1.28	1.058	1.093	1.081	1.058	1.068	1.107	1.122	1.121
1.32	0.891	0.905	0.853	0.949	0.945	0.947	0.955	0.946
1.36	0.781	0.770	0.713	0.872	0.859	0.840	0.824	0.817
1.40	0.699	0.677	0.617	0.818	0.798	0.758	0.739	0.742
1.44	0.650	0.621	0.563	0.778	0.754	0.699	0.682	0.664
1.48	0.616	0.595	0.532	0.751	0.724	0.672	0.640	0.622
1.52	0.606	0.574	0.520	0.742	0.719	0.661	0.627	0.597
1.56	0.612	0.583	0.518	0.741	0.720	0.652	0.625	0.599
1.60	0.631	0.601	0.548	0.759	0.732	0.667	0.644	0.626
1.64	0.663	0.645	0.590	0.782	0.757	0.696	0.677	0.656
1.68	0.720	0.702	0.651	0.817	0.792	0.738	0.725	0.701
1.72	0.790	0.771	0.733	0.863	0.839	0.794	0.781	0.757
1.76	0.873	0.857	0.830	0.913	0.891	0.854	0.854	0.831
1.80	0.960	0.946	0.951	0.967	0.954	0.920	0.930	0.907
1.84	1.040	1.039	1.058	1.019	1.016	0.992	1.009	0.986
1.88	1.113	1.114	1.153	1.075	1.071	1.062	1.079	1.072
1.92	1.180	1.178	1.217	1.118	1.174	1.127	1.137	1.142
1.96	1.221	1.236	1.261	1.143	1.153	1.188	1.191	1.198
2.00	1.250	1.268	1.286	1.156	1.172	1.220	1.231	1.24_0
2.04	1.268	1.284	1.306	1.151	1.180	1.232	1.248	1.267
2.08	1.257	1.277	1.305	1.135	1.165	1.225	1.241	1.269
2.12	1.223	1.248	1.288	1.108	1.131	1.203	1.214	1.246
2.16	1.168	1.194	1.244	1.084	1.097	1.160	1.172	1.207
2.20	1.103	1.132	1.179	1.046	1.064	1.112	1.122	1.151
2.24	1.044	1.066	1.100	1.016	1.029	1.056	1.068	1.090
2.28	0.981	0.994	1.015	0.992	0.998	1.007	1.011	1.021
2.32	0.936	0.934	0.945	0.968	0.969	0.967	0.960	0.967
2.36	0.896	0.890	0.876	0.952	0.946	0.934	0.924	0.923
2.40	0.869	0.851	0.825	0.939	0.930	0.906	0.892	0.881
2.60	0.894	0.878	0.842	0.950	0.937	0.933	0.894	0.876
2.80	1.044	1.046	1.059	1.016	1.016	1.017	1.026	1.023
3.00	1.088	1.101	1.129	1.035	1.045	1.071	1.080	1.095
3.20	1.002	1.006	1.010	1.002	1.005	1.012	1.0_{14}	1.021
3.40	0.941	0.930	0.911	0.980	0.975	0.959	0.951	0.942
3.60	0.978	0.972	0.960	0.992	0.988	0.976	0.974	0.966
3.80	1.0_{32}	1.037	1.051	1.009	1.011	1.017	1.023	1.026
4.00	1.026	1.033	1.047	1.008	1.011	1.023	1.026	1.034
4.20	0.988	0.986	0.981	0.998	0.998	0.997	0.994	0.995
4.40	0.978	0.972	0.959	0.994	0.992	0.984	0.980	0.974
4.60	1.000	0.999	0.992	0.999	0.998	0.996	0.996	0.994
4.80	1.016	1.020	1.029	1.003	1.005	1.009	1.012	1.015
5.00	1.005	1.008	1.012	1.001	1.003	1.006	1.007	1.010

TABLE IV (*continued*)

ρ / T / r	0.850	0.850	0.850	0.824	0.750	0.750	0.750	0.750
	0.786	0.719	0.658	0.820	2.845	1.304	1.070	0.827
0.84	0.000	0.000	0.0000	0.000	0.004	0.000	0.000	0.000
0.88	0.000	0.000	0.0000	0.000	0.104	0.002	0.000	0.000
0.92	0.017	0.010	0.0039	0.020	0.555	0.099	0.048	0.015
0.96	0.324	0.254	0.1315	0.332	1.280	0.618	0.457	0.300
1.00	1.377	1.257	0.8487	1.337	1.823	1.533	1.369	1.050
1.04	2.514	2.491	2.1002	2.422	2.031	2.194	2.168	2.110
1.08	2.938	3.001	2.9569	2.829	1.978	2.362	2.461	2.480
1.12	2.726	2.807	3.0373	2.629	1.810	2.209	2.340	2.610
1.16	2.246	2.327	2.6773	2.220	1.614	1.940	2.036	2.188
1.20	1.794	1.821	2.1735	1.794	1.432	1.661	1.731	1.844
1.24	1.419	1.433	1.6837	1.434	1.270	1.414	1.471	1.526
1.28	1.143	1.145	1.2824	1.179	1.147	1.226	1.248	1.279
1.32	0.938	0.930	0.9919	0.977	1.037	1.076	1.086	1.086
1.36	0.790	0.793	0.7894	0.843	0.954	0.949	0.946	0.954
1.40	0.703	0.694	0.6499	0.745	0.898	0.857	0.857	0.845
1.44	0.634	0.628	0.5575	0.682	0.849	0.806	0.790	0.783
1.48	0.594	0.591	0.5144	0.633	0.823	0.764	0.742	0.722
1.52	0.579	0.564	0.5045	0.618	0.803	0.739	0.713	0.685
1.56	0.581	0.566	0.5175	0.626	0.792	0.728	0.703	0.675
1.60	0.595	0.587	0.5404	0.624	0.796	0.724	0.699	0.677
1.64	0.631	0.623	0.5759	0.649	0.810	0.732	0.716	0.692
1.68	0.681	0.674	0.6081	0.687	0.830	0.758	0.735	0.715
1.72	0.748	0.735	0.6472	0.745	0.855	0.783	0.776	0.750
1.76	0.827	0.820	0.6985	0.812	0.886	0.830	0.814	0.791
1.80	0.916	0.917	0.7857	0.890	0.926	0.880	0.870	0.847
1.84	1.014	1.014	0.9117	0.974	0.965	0.930	0.928	0.914
1.88	1.095	1.090	1.0656	1.056	1.006	0.988	0.980	0.973
1.92	1.160	1.161	1.2184	1.116	1.048	1.044	1.044	1.036
1.96	1.202	1.213	1.3447	1.178	1.079	1.093	1.100	1.087
2.00	1.247	1.252	1.4091	1.224	1.104	1.138	1.141	1.146
2.04	1.275	1.272	1.4166	1.256	1.110	1.161	1.173	1.183
2.08	1.280	1.283	1.3729	1.264	1.108	1.169	1.188	1.202
2.12	1.255	1.268	1.3015	1.244	1.101	1.169	1.181	1.207
2.16	1.223	1.226	1.2201	1.206	1.085	1.149	1.160	1.198
2.20	1.164	1.169	1.1429	1.156	1.062	1.117	1.141	1.167
2.24	1.093	1.099	1.0713	1.097	1.040	1.091	1.107	1.127
2.28	1.025	1.034	1.0051	1.042	1.020	1.055	1.063	1.080
2.32	0.964	0.972	0.9461	0.984	1.004	1.016	1.030	1.035
2.36	0.916	0.916	0.8989	0.936	0.983	0.990	0.994	1.004
2.40	0.869	0.872	0.8766	0.901	0.973	0.962	0.962	0.960
2.60	0.866	0.857	0.853	0.876	0.969	0.923	0.914	0.897
2.80	1.030	1.030	1.031	1.009	0.995	0.985	0.982	0.975
3.00	1.102	1.107	1.110	1.088	1.021	1.041	1.046	1.054
3.20	1.020	1.022	1.022	1.028	1.010	1.026	1.031	1.040
3.40	0.936	0.934	0.932	0.952	0.993	0.986	0.985	0.982
3.60	0.963	0.959	0.958	0.963	0.991	0.979	0.975	0.967
3.80	1.030	1.031	1.032	1.018	1.001	1.000	0.999	0.997
4.00	1.037	1.040	1.041	1.032	1.005	1.013	1.015	1.020
4.20	0.993	0.994	0.993	1.001	1.002	1.006	1.007	1.011
4.40	0.972	0.969	0.968	0.979	0.998	0.994	0.993	0.992
4.60	0.994	0.993	0.993	0.991	0.998	0.994	0.993	0.989
4.80	1.018	1.019	1.020	1.011	1.000	1.001	1.001	1.001
5.00	1.011	1.013	1.013	1.011	1.001	1.004	1.005	1.070

TABLE IV (*continued*)

ρ / T / r	0.650 3.669	0.650 1.827	0.650 1.584	0.650 1.036	0.650 0.900	0.500 1.360	0.450 2.934	0.450 1.710	0.450 1.552
0.84	0.013	0.000	0.000	0.000	0.000	0.000	0.002	0.000	0.000
0.88	0.170	0.015	0.006	0.000	0.000	0.001	0.064	0.007	0.004
0.92	0.640	0.200	0.138	0.034	0.018	0.069	0.353	0.122	0.092
0.96	1.228	0.765	0.658	0.343	0.257	0.428	0.841	0.543	0.498
1.00	1.633	1.457	1.411	1.120	1.016	1.109	1.298	1.169	1.125
1.04	1.776	1.821	1.921	1.892	1.890	1.694	1.551	1.640	1.613
1.08	1.750	2.021	2.076	2.258	2.328	1.961	1.620	1.852	1.837
1.12	1.659	1.922	2.003	2.225	2.335	1.946	1.573	1.828	1.848
1.16	1.526	1.751	1.821	2.024	2.118	1.830	1.504	1.734	1.753
1.20	1.393	1.565	1.608	1.749	1.815	1.658	1.411	1.573	1.604
1.24	1.275	1.405	1.425	1.516	1.545	1.491	1.323	1.439	1.479
1.28	1.166	1.256	1.263	1.326	1.340	1.335	1.241	1.311	1.336
1.32	1.086	1.136	1.145	1.165	1.173	1.227	1.167	1.219	1.219
1.36	1.019	1.032	1.044	1.043	1.044	1.129	1.107	1.139	1.133
1.40	0.958	0.968	0.965	0.959	0.936	1.059	1.051	1.075	1.060
1.44	0.924	0.913	0.906	0.884	0.860	0.982	1.006	1.013	1.006
1.48	0.897	0.866	0.861	0.841	0.809	0.929	0.975	0.968	0.962
1.52	0.875	0.841	0.833	0.801	0.779	0.898	0.959	0.938	0.935
1.56	0.862	0.818	0.805	0.776	0.756	0.881	0.929	0.923	0.916
1.60	0.856	0.808	0.797	0.763	0.744	0.863	0.921	0.907	0.897
1.64	0.859	0.809	0.796	0.764	0.745	0.860	0.913	0.900	0.898
1.68	0.871	0.813	0.805	0.774	0.765	0.859	0.912	0.890	0.885
1.72	0.891	0.827	0.820	0.794	0.775	0.854	0.913	0.893	0.884
1.76	0.907	0.855	0.844	0.822	0.804	0.873	0.925	0.900	0.889
1.80	0.927	0.887	0.873	0.854	0.847	0.894	0.933	0.909	0.906
1.84	0.955	0.916	0.916	0.899	0.891	0.907	0.954	0.923	0.919
1.88	0.982	0.950	0.951	0.934	0.947	0.938	0.965	0.942	0.937
1.92	1.003	0.995	0.991	0.974	0.987	0.966	0.978	0.969	0.959
1.96	1.025	1.032	1.029	1.022	1.039	0.994	0.990	0.989	0.983
2.00	1.040	1.062	1.064	1.064	1.083	1.021	1.005	1.014	1.009
2.04	1.059	1.083	1.087	1.097	1.117	1.047	1.016	1.025	1.022
2.08	1.066	1.096	1.104	1.126	1.144	1.062	1.025	1.044	1.041
2.12	1.064	1.102	1.110	1.139	1.155	1.075	1.023	1.054	1.053
2.16	1.055	1.103	1.101	1.140	1.155	1.082	1.025	1.051	1.061
2.20	1.046	1.087	1.097	1.123	1.137	1.073	1.026	1.051	1.054
2.24	1.036	1.065	1.083	1.102	1.113	1.066	1.022	1.050	1.053
2.28	1.029	1.051	1.056	1.082	1.088	1.056	1.016	1.042	1.046
2.32	1.019	1.028	1.035	1.052	1.055	1.044	1.014	1.028	1.035
2.36	1.005	1.016	1.019	1.024	1.021	1.030	1.009	1.024	1.028
2.40	0.999	1.004	1.001	1.003	0.992	1.022	1.009	1.018	1.011
2.60	0.878	0.961	0.956	0.943	0.934	0.982	0.995	0.990	0.995
2.80	0.991	0.981	0.981	0.967	0.975	0.984	0.993	0.990	0.990
3.00	1.007	1.013	1.015	1.015	1.026	1.004	0.999	1.001	1.000
3.20	1.007	1.016	1.018	1.027	1.029	1.012	1.003	1.007	1.007
3.40	1.000	1.000	0.999	1.000	0.996	1.005	1.002	1.004	1.005
3.60	0.996	0.992	0.990	0.985	0.982	0.982	1.000	1.000	1.001
3.80	0.999	0.996	0.996	0.993	0.995	0.973	0.999	0.999	0.999
4.00	1.001	1.003	1.004	1.005	1.008	1.001	1.000	1.000	1.000
4.20	1.001	1.003	1.004	1.007	1.007	1.002	1.000	1.001	1.001
4.40	1.000	1.000	1.000	1.000	0.998	1.001	1.000	1.001	1.001
4.60	0.999	0.998	0.998	0.996	0.995	1.000	1.000	1.000	1.000
4.80	1.000	0.999	0.999	0.998	0.999	1.000	1.000	1.000	1.000
5.00	1.000	1.001	1.000	1.002	1.002	1.000	1.000	1.000	1.000